DOI 10.1007/s11182-024-03145-w
Russian Physics Journal, Vol. 67, No. 4, April, 2024

INFLUENCE OF SILVER ION CONTENT ON NANOPARTICLE SIZE OBTAINED BY CAVITATION-DIFFUSION PHOTOCHEMICAL REDUCTION

D. I. Shashkov,[1] G. F. Kopytov,[2] A. A. Basov,[1,3] V. V. Malyshko,[3,4] E. V. Barysheva,[3] M. E. Sokolov,[1] A. V. Moiseev,[5] E. E. Esaulenko,[3] N. D. Shapkin,[1] A. N. Korzhov,[1] V. A. Isaev,[1] and A. A. Dorokhova[1,4]

UDC 538.9; 620.3

Photochemical reduction is used to develop many methods of creating biologically active substances and materials consisting of silver nanoclusters, which makes them relevant for science and technology, including different trends in biotechnology, catalytic systems, label-free quantification, metasurfaces and nanohybrid composites. The paper presents the silver nanoparticle (AgNP) technology based on cavitation-diffusion photochemical reduction in the presence of 10 mg of ligand (polyvinylpyrrolidone) allowing to significantly change the AgNP content depending on the concentration of silver nitrate ($AgNO_3$) *in the reaction system, and providing the AgNP domination having a certain size. It is found that at 5 mg of* $AgNO_3$ *in the reaction system, the size of at least 60% of synthesized nanoparticles, is 26 nm or more, while at 2.5 mg of* $AgNO_3$*, up to 94.7% of nanoparticles have the size of 15 nm and less, 6 to 10 nm AgNPs being dominated. This meets the need for AgNPs of a certain the size in different fields of science and technology, including medical and pharmaceutical industries, agriculture, and laboratory diagnostics.*

Keywords: nanoparticle synthesis, silver nanoparticles, polyvinylpyrrolidone, electron microscopy.

INTRODUCTION

The photochemical synthesis of silver nanoparticles (AgNPs) underlies many methods of creating Ag-containing biologically active substances and materials. These nanoparticles can be used in different fields of science and technology, including biotechnology, catalytic systems, and laboratory analysis [1–3]. For example, plasmonic silver nanoparticles are extremely promising for creating label-free methods for recording disease markers in body fluids, identifying pathogens in food and various chemicals during environmental monitoring of objects. The latter can be provided by multicolor biosensors and chemosensors, significantly improving the observation accuracy. Since the wavelength absorbed by nanoparticles is affected by their size, shape, orientation, and distance between them, it is advisable to use the cyclic oxidation process of silver atoms in AgNPs for creating highly sensitive elements, as it changes the ratio, shape and plasmon peak [4]. This approach combined with the AgNP-based electrochemical sensor readout allows to overcome limitations of traditional colorimetric systems [5]. Moreover, a combination of different nanostructures, for example, Ag-containing spherical particles and Au-containing anisotropic particles with several sharp edges like nanoflowers [6], allows to create structures (primarily dimers of plasmonic nanoparticles) with the

[1]Kuban State University, Krasnodar, Russia, e-mail: shinix88@mail.ru; sokolovme@mail.ru; kolyasfg123@mail.ru; shtrih_ooo@mail.ru; vlisaev.v@yandex.ru; [2]Razumovsky Moscow State University of Technology and Management, Moscow, Russia, e-mail: g137@mail.ru; [3]Kuban State Medical University, Krasnodar, Russia, e-mail: son_sunytch79@mail.ru; baryshev_mg@mail.ru; esaulenkoe@bk.ru; [4]Southern Scientific Center of the Russian Academy of Science, Rostov-on-Don, Russia, e-mail: intro-2@rambler.ru; 013194@mail.ru; [5]Kuban State Agrarian University, Krasnodar, Russia, e-mail: moiseew_a@rambler.ru. Original article submitted March 17, 2024.

properties suitable for universal labels for surface-enhanced Raman scattering and substrate components for single-molecule surface-enhanced Raman scattering measurements, that is implemented by placing dye molecules into hot spots located in interparticle spaces ranging in size of 1 to 3 nm [7].

Lafitte *et al*. [8] report that silver nanoclusters are characterized by pronounced stability, which provides great promise for using them in optics to obtain metasurfaces. Silver nanoclusters are two-dimensional assemblies of nanoscale optical resonators considered as a next generation of ultrathin optical components applied in the manufacture of complex colloidal resonators possessing both magnetic and electrical resonances. It is proven that these structures can be obtained by the homogeneous film deposition, including water suspension emulsification of silver nanoparticles in the oil phase followed by controlled emulsion drying and formation of colloidal silver clusters. Metasurfaces obtained in this way, consist of homogeneous films of variable surface density and colloidal clusters. It is also possible to use nanofilaments and silver nanoparticles to create flexible organic light-emitting diodes possessing extraordinary mechanical flexibility, excellent optoelectronic properties, and high mechanical stability [9]. It is shown that even after 500 flexure tests, the brightness of flexible and transparent electrodes modified by silver nanostructures, is at least 82% of the initial value.

Recently, silver nanoparticles are being widely used for biotech platform assemblies allowing a prolonged use of antimicrobial substances. In particular, antibacterial microstructures (microneedles) are obtained with controlled release of microbicidal components based on polylactide and silver nanoparticles in the proportion of 1 to 5%. At the same time, their production for medical purposes is based on micro-molding from the prepared solution. According to Chamgordani *et al*. [10], these microstructures show good mechanical strength without signs of fracture while maintaining the optimum concentration of the antibacterial (Ag^+) substance for 34 days. Various fields of the Ag nanostructure application, are attributed to modified physicochemical properties of nanoparticles, namely shape, size, composition [11, 12]. The latter can be achieved due to both qualitatively different components and quantitative characteristics of substrates used during the AgNP synthesis [13, 14]. To obtain nanoparticles of a certain size, shape, composition and structure, special synthesis methods are developed, including physical, chemical and photochemical factors, the latter being more preferable [15–17]. This is stipulated by the fact that photochemical reduction leads to the lowest quantity of byproducts, requires no complex equipment and high synthesis temperatures, is characterized by lower energy necessary for the reaction, and provides a precise space-time control for the rate and reduction of silver ions [18]. In optimizing the nanoparticle synthesis by the photochemical reduction, it is important to select the reagent concentration in the reaction system. For example, Pacheco *et al*. [19], indicate that the use of sodium borohydride as a reducing agent and polyvinylpyrrolidone stabilizer, leads to the higher content (<10 nm) of ultra-fine AgNPs with almost spherical shape (low anisotropy) and, among other things, low dispersion at their certain concentration at a fixed molar ratio of 1 to 2 of $AgNO_3$ and $NaBH_4$, respectively.

The aim of this work is to study changes in the AgNP size range obtained by cavitation-diffusion photochemical reduction at different concentrations of silver nitrate in the reaction system.

MATERIALS AND METHODS

The equipment and installations of the Core Facility Center for Nanomaterial Structure and Property Diagnostics of Kuban State University (Krasnodar, Russia) were used in the experiment. The obtained silver nanoparticles were studied by electron microscopy using freshly prepared solutions. The aqueous nanoparticle solution was obtained by cavitation-diffusion photochemical reduction, that involved the Ag^+ reduction in the presence of polyvinylpyrrolidone [20]. Silver nanoclusters were obtained under a combined action of ultrasonic waves (1.7 MHz radiation frequency) and ultraviolet radiation for 1 hour [21]. The nanoparticle size, quantity, and shape were evaluated after the addition of 2.5 and 5 mg of silver nitrate at the same (10 mg) polyvinylpyrrolidone concentration. Ultrasound and ultraviolet radiation parameters were the same for both series of the experiment. The AgNP size was compared with the reference marker 100 nm long [22]. Variation statistics methods were used to verify the experimental data. Validation of differences between AgNPs in different size ranges was performed using the Mann–Whitney *U* test. The significant difference was $p < 0.05$.

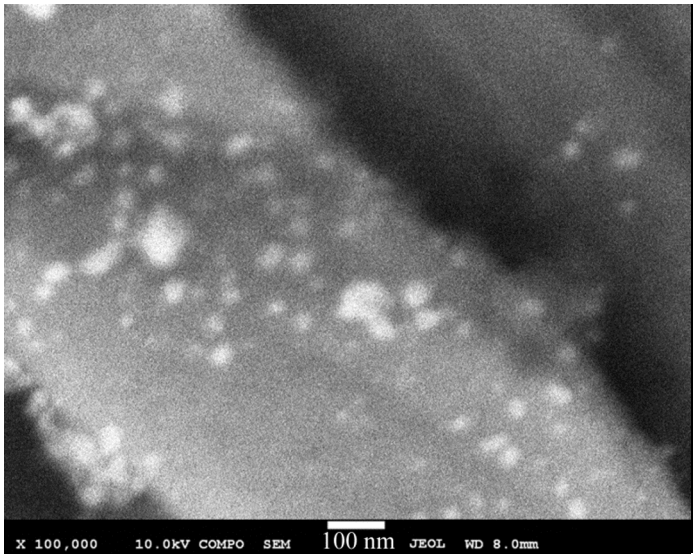

Fig. 1. SEM backscattered-electron image of nanoparticle solution. Silver nitrate: 5 mg. Magnification: 100,000×.

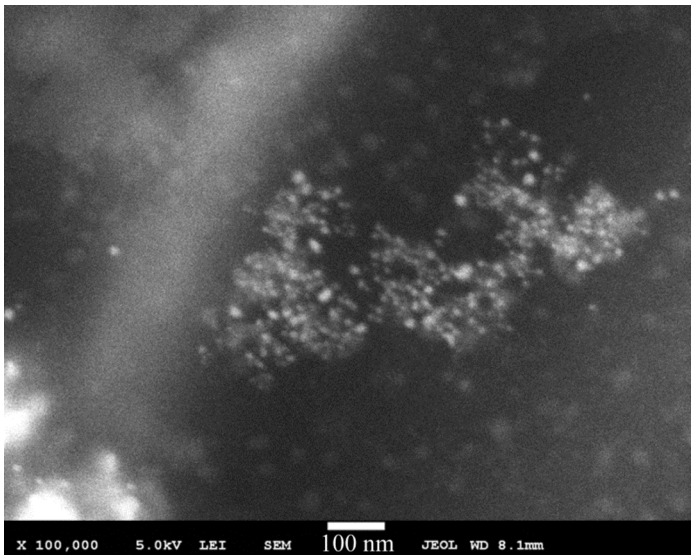

Fig. 2. SEM backscattered-electron image of nanoparticle solution. Silver nitrate: 2.5 mg. Magnification: 100,000×.

RESULTS AND DISCUSSION

The experiment showed that at the silver nitrate ($AgNO_3$) concentration reduced by 2 times, the number and size of synthesized AgNPs significantly changed. Multidirectional shifts were observed during the AgNP formation in groups of >15 nm and <25 nm nanoparticles, which was accompanied by a decrease in the number of coarse silver nanoparticles and an increase in the number of the most functionally active nanoclusters of a smaller size, as shown in Figs. 1, 2.

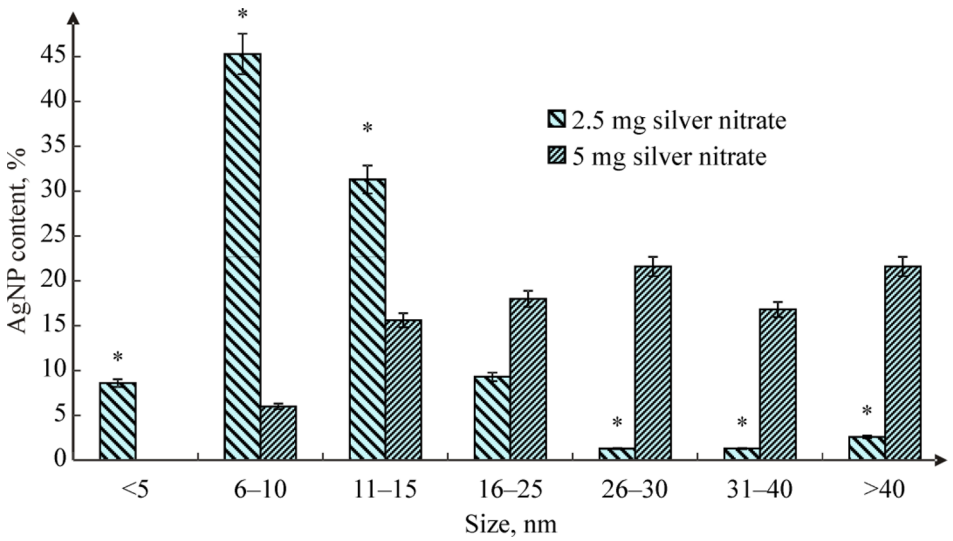

*Statistically significant difference in the AgNP content of comparable size range ($p < 0.05$) from that in the reaction mixture with 5 mg of $AgNO_3$. 100% corresponds to 83 and 151 AgNPs at 5 and 2.5 mg of $AgNO_3$, respectively.

Fig. 3. AgNPs of different size at different $AgNO_3$ concentration during the synthesis process.

It is known that the synthesis of functionally active nanoparticles with the size not over 15 nm, is interesting for various fields of medicine and technology. For example, in dentology and surgery, such nanoparticles are effective when used as an antibacterial component of wound coverings and anti-infective agents for neutralizing gram-negative microorganisms [14, 23]. Moreover, they possess antiviral properties preventing virus replication and a powerful fungicidal effect [24]. Nanoparticles ranging from 15 to 30 nm, have rather high photocatalytic activity due to the formation of reactive oxygen species and are more effective for laboratory diagnostics as a biosensor element [25].

When during the synthesis, the $AgNO_3$ concentration is reduced by 2 times, the number of ≤5 nm AgNPs ($p < 0.05$) significantly grows, whereas in adding 5 mg $AgNO_3$ to the reaction system, AgNPs are not detected at all. As can be seen in Fig. 3, the amount of ≤5 nm AgNPs is 8.6% of their total number. One can see that the number of nanoclusters increases by 13.6 times ($p < 0.05$) in the size range of 6 to 10 nm, when 2.5 mg $AgNO_3$ is added to the reaction system. The similar dynamics is observed for AgNPs ranging from 11 to 15 nm, i.e., their number grows by more than 10.1 times ($p < 0.05$) as compared to their content after the synthesis with 5 mg of $AgNO_3$.

According to SEM backscattered-electron images, the total number of AgNPs ranging between 16 and 25 nm, remains unchanged when synthesized with the different content of silver nitrate ($p > 0.05$), despite the different AgNP percentage, which is almost twice as large in adding 5 mg of $AgNO_3$ than in adding 2.5 mg of $AgNO_3$ (see Fig. 3). At a lower $AgNO_3$ concentration, the opposite dynamics of the larger nanoparticle formation is observed in all size ranges (>25 nm), which is accompanied by a decrease in their proportion from 60 to 5.2% of the total number in the prepared colloidal solution. In adding 2.5 mg of $AgNO_3$ to the reaction system, the content of nanoparticles ranging from 26 to 30 nm, drops by more than 16.5 times, and their absolute number – by 9.2 times ($p < 0.05$) as compared to their content after the addition of 5 mg of $AgNO_3$. The content of nanoparticles ranging from 31 to 40 nm, drops by 12.9 times, and their absolute number – by 7.1 times ($p < 0.05$), whereas for >40 nm nanoparticles, this drop is 8.3 and 4.6 times ($p < 0.05$), respectively.

At a 2-fold decrease in the $AgNO_3$ concentration in the reaction system, the number of fine (≤15 nm) AgNPs obtained by cavitation-diffusion photochemical reduction, significantly grows ($p < 0.05$), while the number of >25 nm AgNPs reduces ($p < 0.05$) and does not exceed 5.3% of the total AgNP content in the synthesized colloidal solution (see Fig. 3).

CONCLUSIONS

The experimental data demonstrated a significant modification of final products of photochemical reduction *via* changes in the reagent concentration in the reaction mixture to produce AgNPs of a certain size and their further application in different fields of science and technology.

It is advisable to use fine (<16 nm) AgNPs in medicine as, for example, an antimicrobial agent, since they constitute up to 94.7% at a 2-fold decrease (down to 2.5 mg) in the $AgNO_3$ concentration and constant concentration of the reducing agent and ligand. This is stipulated by the ability of fine AgNPs to provide greater contact with bacterial cells for their easier absorption. All this ensures the nanoparticle adhesion through electromagnetic interactions, when the positive charge on the outside of the nanocluster contacts with the negative electrical charge of the cell membrane of a bacterium or fungal cell, thus improving the nanoparticle adhesion to the membrane, followed by penetration into the pathogenic microorganism. The antimicrobial effect can further be achieved also by the Ag^+ release, which attach to cytoderm proteins, causing irreversible structural changes in cell membranes and death of pathogens. Nanoclusters can also bind to mitochondrial and nucleic acids, causing their damage and preventing microbial cell division [26].

Coarse AgNPs obtained *via* the increase in the $AgNO_3$ concentration up to 5 mg constituting over 60%, can be used, for example, in agriculture. Negatively charged AgNPs ranging from 30 to 60 nm, demonstrated the most beneficial effect on soil microbiota. They increased the number of microorganisms with beneficial properties (nitrogen-fixing bacteria, lignin-degrading microbes) [27]. Moreover, coarse (~60 nm) AgNPs immobilized in a chitosan film, can be used for reproducible, sensitive, label-free quantitation of β-amyloid aggregates in diagnostics of early stages of neurodegenerative diseases [28]. Also, these nanoparticles can be employed for the surface functionalization, for example, to improve the photocatalyst efficiency fecilitating a wide use of various nanohybrids [29].

The proposed synthesis of silver nanoparticles using cavitation-diffusion photochemical reduction in the presence of 10 mg of polyvinylpyrrolidone allowed to significantly change the AgNP size range, *viz*. from 60% of ≥26 nm nanoparticles (at 5.0 mg of $AgNO_3$) to 94.7% of ≤15 nm nanoparticles (at 2.5 mg $AgNO_3$), that meets the needs of science and technology, including medical and pharmaceutical industries, agriculture, and laboratory diagnostics.

COMPLIANCE WITH ETHICAL STANDARDS

Author contributions

Conceptualization A. A. B.; methodology V. V. M. and D. I. Sh.; formal analysis E. E. E., M. E. S., and E. V. B.; writing—original draft preparation A. A. B, V. V. M., and A. A. D.; writing—review and editing A. V. M., V. A. I., and D. I. Sh.; visualization N. D. Sh. and A. N. K.; supervision G. F. K.

All authors have read and agreed to the published version of the manuscript.

Conflict of interest

The authors declare no conflict of interest.

Financial interests

The authors declare they have no financial interests.

Funding

This work was carried out under the government contract No. FZEN-2023-0006 of the Ministry of Science and Higher Education of the Russian Federation.

REFERENCES

1. D. Samal, P. Khandayataray, M. Sravani, and M. K. Murthy, Environ. Sci. Pollut. Res. Int., **31**, No. 6, 8400 (2024); DOI: 10.1007/s11356-023-31669-0.
2. Y. R. Lai, J. T. Lai, S. S. Wang, Y. C. Kuo, and T. H. Lin, Int. J. Biol. Macromol., **213**, 1098 (2022); DOI: 10.1016/j.ijbiomac.2022.06.016.
3. I. S. Petriev, M. G. Baryshev, K. A. Voronin, I. S. Lutsenko, P. D. Pushankina, and G. F. Kopytov, Russ. Phys. J., **63**, 457 (2020); DOI: 10.1007/s11182-020-02056-w.
4. M. Zhilnikova, E. Barmina, G. Shafeev, A. Vasiliev, and I. Pavlov, J. Phys. Chem. Sol., **160**, 110356 (2022); DOI: 10.1016/j.jpcs.2021.110356.
5. E. T. Athira and J. Satija, Analyst, **148**, No. 24, 6188 (2023); DOI: 10.1039/d3an01244a.
6. I. Petriev, P. Pushankina, G. Andreev, S. Ivanin, and S. Dzhimak, Int. J. Mol. Sci., **24**, No. 24, 17403 (2023); DOI: 10.3390/ijms242417403.
7. Y. Kanehira, K. Tapio, G. Wegner, S. Jr. Kogikoski, S. Rüstig, C. Prietzel, K. Busch, and I. Bald, ACS Nano, **17**, No. 21, 21227 (2023); DOI: 10.1021/acsnano.3c05464.
8. M. Lafitte, R. Dwivedi, R. Elancheliyan, F. Lagugné-Labarthet, L. Buisson, I. Ly, P. Barois, A. Baron, O. Mondain-Monval, and V. Ponsinet, Langmuir, **40**, No. 5, 2601 (2024); DOI: 10.1021/acs.langmuir.3c02900.
9. Z. Wu, X. Xing, Y. Sun, Y. Liu, Y. Wang, S. Li, and W. Wang, Materials (Basel), **17**, No. 2, 505 (2024); DOI: 10.3390/ma17020505.
10. N. Z. Chamgordani, S. Asiaei, F. Ghorbani-Bidkorpeh, M. Babaee Foroutan, A. Mahboubi, and H. R. Moghimi, Drug Deliv. Transl. Res., **14**, No. 2, 386 (2024); DOI: 10.1007/s13346-023-01406-8.
11. P. Pushankina, M. Baryshev, and I. Petriev, Nanomaterials, **12**, No. 23, 4178 (2022); DOI: 10.3390/ nano12234178.
12. S. M. Pridvorova, M. I. Zhilnikova, E. V. Barmina, and G. A. Shafeev, Phys. Wave Phenom., **29**, No. 1, 47 (2021); DOI: 10.3103/S1541308X21010052.
13. B. Pascu, A. Negrea, M. Ciopec, N. Duteanu, P. Negrea, L. A. Bumm, O. G. mBuriac, N. S. Nemeş, C. Mihalcea, and D. M. Duda-Seiman, Int. J. Mol. Sci., **24**, No. 1, 255 (2022); DOI: 10.3390/ijms24010255.
14. A. Basov, S. Dzhimak, M. Sokolov, V. Malyshko, A. Moiseev, E. Butina, A. Elkina, and M. Baryshev, Nanomaterials, **12**, No. 7, 1164 (2022); DOI: 10.3390/nano12071164.
15. J. Benalcázar, E. D. Lasso, C. M. Ibarra-Barreno, J. A. Arcos Pareja, N. S. Vispo, J. C. Chacón-Torres, and S. Briceño, ACS Omega, **7**, No. 50, 46745 (2022); DOI: 10.1021/acsomega.2c05793.
16. G. F. Kopytov, D. I. Shashkov, A. A. Basov, V. V. Malyshko, M. E. Sokolov, A. P. Storozhuk, A. V. Moiseev, A. M. Barysheva, N. V. Zubova, V. A. Isaev, and A. A. Dorokhova, Russ. Phys. J., **67**, 156 (2024); DOI: 10.1007/s11182-024-03102-7.
17. I. S. Petriev, I. S Lutsenko., P. D. Pushankina, V. Yu. Frolov, Yu. S. Glazkova, T. I. Mal'kov, A. M. Gladkikh, M. A. Otkidach, E. B. Sypalo, P. M. Baryshev, N. A. Shostak, and G. F. Kopytov, Russ. Phys. J., **65**, No. 2, 312 (2022); DOI: 10.1007/s11182-022-02637-x.
18. E. Urzúa, F. Gonzalez-Torres, V. Beltrán, P. Barrias, S. Bonardd, A. M. R Ramírez, and M. Ahumada, Nanoscale Advances, **4**, No. 22, 4789 (2022); DOI: 10.1039/d2na00539e.
19. P. G. F. Pacheco, D. L. Ferreira, R. S. Pereira, and M. G. Vivas, Analyst, **148**, No. 20, 5262 (2023); DOI: 10.1039/d3an01319g.
20. S. S. Dzhimak, M. E. Sokolov, A. A. Basov, S. R. Fedosov, V. V. Malyshko, R. V. Vlasov, O. M. Lyasota, and M. G. Baryshev, Nanotechnol. Russ., **11**, 835 (2016); DOI: 10.1134/S1995078016060082.
21. S. S. Dzhimak, V. V. Malyshko, A. I. Goryachko, M. E. Sokolov, A. V. Moiseev, and A. A. Basov, Nanotechnol. Russ., **14**, 48 (2019); DOI: 10.1134/S199507801901004X.
22. S. S. Dzhimak, V. V. Malyshko, A. I. Goryachko, M. E. Sokolov, A. A. Basov, A. V. Moiseev, D. I. Shashkov, G. F. Kopytov, M. G. Baryshev, and V. A. Isaev, Russ. Phys. J., **62**, No. 2, 314 (2019); DOI: 10.1007/S11182-019-01714-Y.

23. A. A. Basov, S. R. Fedosov, V. V. Malyshko, A. A. Elkina, O. M. Lyasota, and S. S. Dzhimak, J. Wound Care, **30**, 312 (2021); DOI: 10.12968/jowc.2021.30.4.312.
24. A. Gibała, P. Żeliszewska, T. Gosiewski, A. Krawczyk, D. Duraczyńska, J. Szaleniec, M. Szaleniec, and M. Oćwieja, Biomolecules, **11**, No. 10,1481 (2021); DOI: 10.3390/biom11101481.
25. I. M. Bykov, A. A. Basov, V. V. Malyshko, S. S. Dzhimak, S. R. Fedosov, and A. V. Moiseev, Bull. Exp. Biol. Med., **163**, No. 2, 268 (2017); DOI: 10.1007/s10517-017-3781-3.
26. S. Khursheed, J. Dutta, I. Ahmad, M. A. Rather, I. A. Badroo, T. A. Bhat, I. Ahmad, A. Amin, A. Shah, T. Qadri, and H. Habib, Food Chem. X, **20**, 101051 (2023); DOI: 10.1016/j.fochx.2023.101051.
27. S. W. Przemieniecki, K. Ruraż, O. Kosewska, M. Oćwieja, and A. Gorczyca, Sci. Total Environ., **914**, 169824 (2024); DOI: 10.1016/j.scitotenv.2023.169824.
28. O. E. Eremina, N. R. Yarenkov, G. I. Bikbaeva, O. O. Kapitanova, M. V. Samodelova, T. N. Shekhovtsova, I. E. Kolesnikov, A. V. Syuy, A. V. Arsenin, V. S. Volkov, G. I. Tselikov, S. M. Novikov, A. A. Manshina, and I. A. Veselova, Talanta, **266**, No. 1, 124970 (2024); DOI: 10.1016/j.talanta.2023.124970.
29. D. R. Mota, W. D. S. Martini, and D. S. Pellosi, Environ. Sci. Pollut. Res. Int., **30**, No. 20, 57667 (2023); DOI: 10.1007/s11356-023-26580-7.